行政院國家科學委員會專題研究計畫　成果報告

多孔性球型燃燒器火燄及流場穩定性實驗與數值分析(2/2)

計畫類別：個別型計畫
計畫編號：NSC94-2212-E-009-007-
執行期間：94 年 08 月 01 日至 95 年 07 月 31 日
執行單位：國立交通大學機械工程學系(所)

計畫主持人：陳俊勳

計畫參與人員：陳俊勳

報告類型：完整報告
報告附件：出席國際會議研究心得報告及發表論文
處理方式：本計畫可公開查詢

中　華　民　國 95 年 9 月 18 日

摘要

本實驗是研究進氣速度(U_{in})與甲烷-氮氣質量比(α)，固定噴油速度(0.05 m/sec)在風洞中單多孔性圓柱燃燒器對火焰轉換現象。實驗過程中先固定燃料之甲烷-氮氣質量比再改變進速度 0.41 至 2.63 m/sec 來觀察相關的火焰結構變化。在實驗中發現在甲烷-氮氣質量比例在高於$\alpha > 60\%$，當進氣速度增加時火焰結構變化由包封火焰、轉換火焰、尾焰依序出現。轉換區存在於包封火焰與尾焰之間。在此區域火焰呈現一來回擺動的特徵且只存在 5~8 秒。在此區域火焰為高度不穩定它可以是一個昇離火焰、尾焰或是熄滅。在另一方面當甲烷-氮氣質量比例在低於 60%，當進氣速度逐漸增加至極限值時火焰由包封焰直接轉變為尾焰並且沒有轉換火焰存在於此區域。這實驗觀測的趨勢與相關數值模擬的結果，有定性的相似。

ABSTRACT

This experimental study investigates the flame transition phenomena over a single Tsuji burner as functions of the incoming flow velocity (U_{in}) and methane to nitrogen mass ratio (α) under a fixed fuel blowing velocity (0.05m/sec) in a wind tunnel. The experimental process is that it fixes the assigned composition of fuel firstly, then, changes the incoming velocity from 0.41 to 2.63 m/sec to observe the corresponding flame configuration. From the experimental observation, in the higher methane mass fraction regime, ($\alpha > 60\%$), the envelope, transition and wake flames appear in order as the incoming flow velocity increases. A transition zone between envelop and wake flame regions is identified in this regime. In such zone, the flame shows an oscillatory feature and can only be survived for 5~8 seconds. It is highly unstable that it might appear as a lift-off flame, wake flame or extinction. On the other hand, when $\alpha \le 60\%$, the envelope flame is directly transformed into wake one as incoming velocity gradually increases up to the transition velocity, and no transition flame is identified in this regime. The observed trend is similar qualitatively to the corresponding predicted one.

1. Introduction

This study is to observe the flame structure transitions and measure temperature distributions along the vertical centerline of a single Tsuji burner at a fixed cylinder surface fuel-ejection velocity, V_w = 5 cm/s, ejected from the forward half part of the burner. The varying parameters are the incoming airflow velocity, U_{in}, and the methane to nitrogen ratio, α, in the ejection mixture. The purpose is to understand the physical mechanism for the flame transition over a Tsuji burner and dilution effects of nitrogen Basically, the present study is an extension and modification of Chang's experiment [1], which used 99.99% methane (CH_4) as the fuel from the Tsuji burner. In this work, the major improvement is to employ a gas mixer to generate the assigned mixture of nitrogen and methane and the instrumentation in test section to measure the flame temperature. Those will be described later.

2. Literature Review

Chang [1] built a wind tunnel to observe the flame lift-off phenomena over a porous burner and further to explain the flame configurations and transition processes by using a series of photographs. The primary parameters in the experiment were the incoming airflow velocity and fuel ejection velocity, respectively. There were two ejection areas, the half fuel ejection area and the full ejection one, under consideration. For the case of the half fuel ejection area, he found that the stand–off distance decreases and flame length increases with an increase of inflow velocity due to the greater flame stretch effect when fuel ejection rate is fixed. As the increase of inflow velocity, the envelope, wake, side, lift-off and late wake flames appeared in order. However, with a higher fixing fuel ejection rate, the envelope flame directly is transformed into lift-off flame without the appearance of wake flame as inflow velocity increases.

Chen [2] further discussed the relationship between the resultant flames and the corresponding cold flow field without combustion. The smoke-generation technique by using oil spread over a heated wire and the laser-sheet lighting system were used to visualize the cold flow field around porous cylindrical burner in a wind tunnel. She found that in a critical incoming flow velocity, the wake is getting more and more closer to the rear surface of cylinder under a fixed fuel ejection velocity when Re is increased. It might be attributed to the pressure distribution of the flow field. When the static pressure of the downstream wake is greater than the one caused by the blowing over the cylinder surface, the wake is pressed back to the rear of cylinder surface.

Tsuji and Yamaoka [3] studied the laminar counterflow diffusion flame

established in the forward stagnation region of a porous cylinder. The flame stability limits and positions as well as the temperature distributions are examined. Two mechanisms for blow-off were identified, namely, the thermal quenching and the flame stretch in flame zone. The critical stagnation velocity gradient is found to depend on the fuel composition, and the fuel composition value can be used as a measure of the over all reaction rate for each combination of reactants. Later, Tsuji and Yamaoka [4] examined the chemical structure and the blow-off mechanism of the laminar counterflow diffusion flame. The concentration distribution of various stable species was measured by a microprobe sampling technique, and the gas-chromatography was used to analyze hydrocarbon flames under various aerodynamic conditions. The overall flame structure was examined by optical interferometer. The flame approaches the cylinder surface when the fuel-ejection rate decreases or stagnation velocity gradient increases. Differences between the concentration profiles in the case of a low fuel-ejection rate and in the case of a large stagnation velocity gradient velocity gradient are significant.

Tsuji and Yamaoka [5] further analyzed the structure of the counterflow diffusion flame, generated in the forward stagnation region of a porous cylinder, and explicated the properties of such diffusion flame. Velocity, temperature, and stable species concentration profiles were measured in detail for methane flames at atmospheric pressure under various aerodynamic conditions. They were determined by two aerodynamic parameters, the non-dimensional fuel-ejection rate, $-f_w$, and the stagnation velocity gradient, $2U_{in}/R$. These distributions were analyzed to determine the reaction-rate profiles of stable species and the heat-release-rate profiles throughout the flame zone. When $-f_w$ becomes very small, the flame approaches the cylinder surface and both the reaction rates and the heat-release rates decrease considerably, implying that these phenomena might be attributed to thermal quenching of the flame.

In the experiment of Tsuji and Yamaoka [6], they adopted methane-air and methane-hydrogen-air mixtures, which both were diluted with nitrogen, as ejecting fuels to investigate the flame behaviors in the counterflow regions. They found that the concentration percentages of nitrogen influence extinction limits. Over the whole range of equivalence ratio, the maximum allowable nitrogen concentration and extinction limit are slant to the fuel-lean side, where equivalence ratio is less than one.

Tsuji and Ishizuka [7] studied a counterflow diffusion flame established in the forward stagnation region of a porous cylinder. The fuels used were methane and hydrogen, and three inert gases, such as nitrogen, argon, and helium were used as the diluents. As the uniform oxidizer stream velocity was increased or mixture ejection velocity was decreased, the flame approached the cylinder and finally blew off from the forward stagnation region. As the fuel concentration in the ejected mixture or

oxygen concentration in the oxidizer stream was decreased, the flame luminosity became weak, and finally the flame blew off.

Dirk et al. [8] utilized Tsuji burner to study the effects of air preheating and simultaneous dilutions of fuel and air stream with nitrogen, argon, and carbon dioxide on the critical strain rate. The air temperature was varied in the wide range from ambient temperature (285 K) to as high as 1500 K. The critical strain rate, $\frac{2V_{air}}{R}\left(1+\frac{V_{F,-\infty}}{V_{air,\infty}}\sqrt{\frac{\rho_{F,-\infty}}{\rho_{air,\infty}}}\right)$, for extinction of methane-air diffusion flame in preheated air was measured. When air is diluted to various degrees with argon, carbon dioxide, or nitrogen, the critical strain rates increase exponentially with air temperatures. The obtained critical strain rates from experiments for methane-air diffusion flames in preheated air were reported for air temperature up to 1500 K. Because it was significantly higher than the auto-ignition temperature of stoichiometry methane-air mixture, the extinction occurred for all temperatures.

3. Experimental Apparatus and Operation Procedure

3.1 Experimental Apparatus

Basically, the present experimental apparatus is same as that in Chang. [1], except a gas mixer is added to generate desired methane-nitrogen mixture. The experimental setup consists of three major elements, which are the wind tunnel, gas mixer and Tsuji burner. Its schematic configuration is shown in Fig. 1.

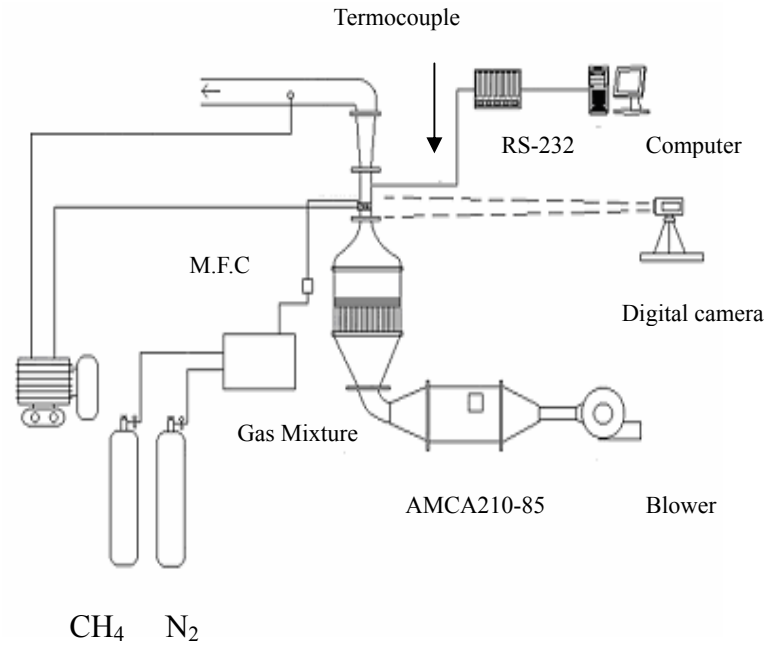

Figure 1. Schematic drawing of overall experimental system

The wind tunnel is designed to provide a laminar, uniform oxidizer flow to the porous cylindrical burner. It is open-circuit and orientated vertically upwards.

The porous cylindrical burner is comprised of inner and outer parts. The diameter of the inner part is 20±0.5 mm, and that of outer part is 30±0.5 mm. The inner part is a cylindrical brass rod with internal water-cooling and fuel supply grooves. The outer part is made of porous sintered stainless steel (20μm pores), and it is a replaceable piece with a length of 40±0.5 mm. The outer part is screwed onto the inner one.

The function of gas mixer is to mix the methane with nitrogen well in an assigned concentration.

3.2 Operation Procedure

During the experiment, as shown in Figure 1. fuel, supplied from a gas mixer, goes through the Tsuji burner and is ejected from its forward half part at a fixed velocity of $v_w = 5cm/s$. For safety reason, the ignition is taken at lower inflow speed to generate a flame, then, it is increased to the assigned flow velocity. The main purpose of this action is to obtain an enveloped stable flame initially. It is worth noting that the ignition device should be operated before the fuel supply valve is open; otherwise it may cause an explosion. Then, the ignition device is removed to avoid the interference with inflow. Eventually, the blower is adjusted to generate a desired flow velocity, and the resultant flame configurations are observed from the frontage of test section and recorded by a digital video camera in the whole process.

Performing this experiment, we found that the flame transition limits will be larger if we don't measure them until the front and back walls of the test section are cooled completely. The discrepancy can be up to 0.3 m/s. Besides, between 6~18 seconds after ignition, the discrepancy is found to be about 0.2 m/s per 6 seconds. This is because that the incoming flow has been preheated in advance. As a consequence, the flame transitions will be delayed. This phenomenon was explained by Jiang et al. [9]. Although, we have measured the flame transition limits individually, the transient time from the ignition to the desired incoming velocity will take approximately 6~9 seconds. Hence, the preheated effect can not be avoided.

4. Results And Discussion

The experimental work mainly investigates the flame transition processes as the functions of nitrogen mass concentration in the gaseous fuel and incoming velocity over a single Tsuji burner. The ejection velocity of methane/nitrogen mixture from

the forward half surface of burner is fixed at ejection 0.05 m/s. However, the actual experimental process is that it fixes the assigned composition of fuel firstly, then, changes the incoming velocity, from 0.41 to 2.63 m/sec, to observe the corresponding flame configuration. The same procedure is carried out again when another fuel composition is taken into consideration.

4.1 Flame Structure Analyses

Fig.2 is used to illustrate the structures of envelop, lift-off and wake flames under 100% methane in fuel (no nitrogen). The flames surrounding the porous cylinder and spreading to downstream in the low-speed flow regime, from 0.41 to 1.24 m/sec, are shown in Figs. 4.2(a) and 4.2(b). such the flame is defined as envelope flame. When the inflow velocity increases up to 1.26 m/sec, the flame front is broken suddenly and is retreated to far downstream of the rear surface of the cylindrical burner. It is defined as flame transition region (see Fig. 3), whose flame configurations are shown in Figs. 2(c) and 2(d). In this region, the lift-off flame front in the range of Uin between 1.24 to 1.53 m/ sec oscillates back-and-forth without a specified frequency because the balance position changes all the time and it can only survive for 5 to 8 seconds. When the inflow velocity exceeds 1.56 m/sec, the flame front retreats along the cylinder surface, then the flame front can stabilize on the rear part of the cylinder as shown in Figs. 2(e) and2(f). Its existing range is from Uin = 1.56 to 2.63 m/s. The ejecting fuel from the forward burner surface is mixed with the incoming oxidizer to make up a flammable mixture, which is carried to downstream and subsequently ignited by the recirculated hot gas behind the cylinder to initiate the reaction to form the wake flame.

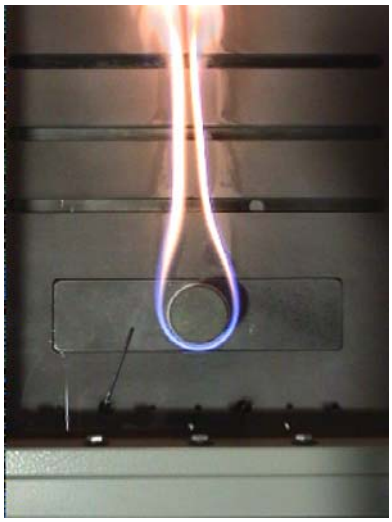

（a）U_{in} = 0.41m/sec

（d）U_{in} = 1.53m/sec

（b）U_{in} = 1.24m/sec

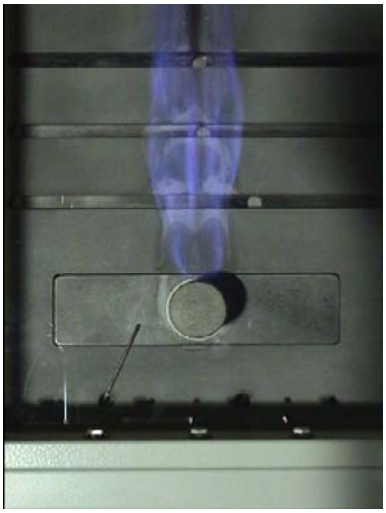

（e）U_{in} = 1.56m/sec

（c）U_{in} = 1.26m/sec

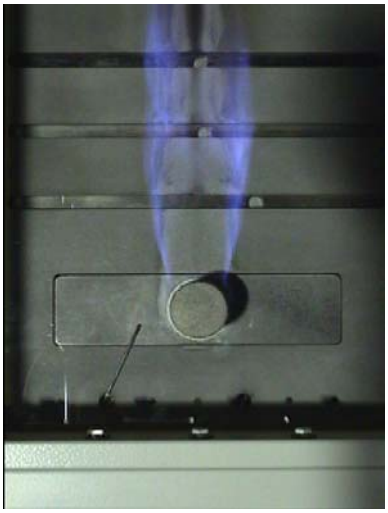

（f）U_{in} = 2.63m/sec

Fig. 2 Series of the pure methane flame configurations as function of inflow velocity from high to low.

4.2 Flame Transition Trend

The ordinate is the incoming velocity, whereas the abscissa is the mass fraction of methane in the methane/nitrogen fuel mixture (α), which is defined as follows.

$$Y_{CH_4} = \frac{X_{CH_4} \times M_{CH_4}}{X_{CH_4} \times M_{CH_4} + X_{N_2} \times M_{N_2}} = \frac{X_{CH_4} \times M_{CH_4}}{X_{CH_4} \times M_{CH_4} + (1 - X_{CH_4}) \times M_{N_2}}$$

$$= \frac{16.04 \times X_{CH_4}}{28.016 - 11.976 X_{CH_4}} = \alpha$$

Note that it reassigns Y_{CH_4} as α here.

Fig. 3 depicts the resultant flame structures as functions of U_{in}, and α.

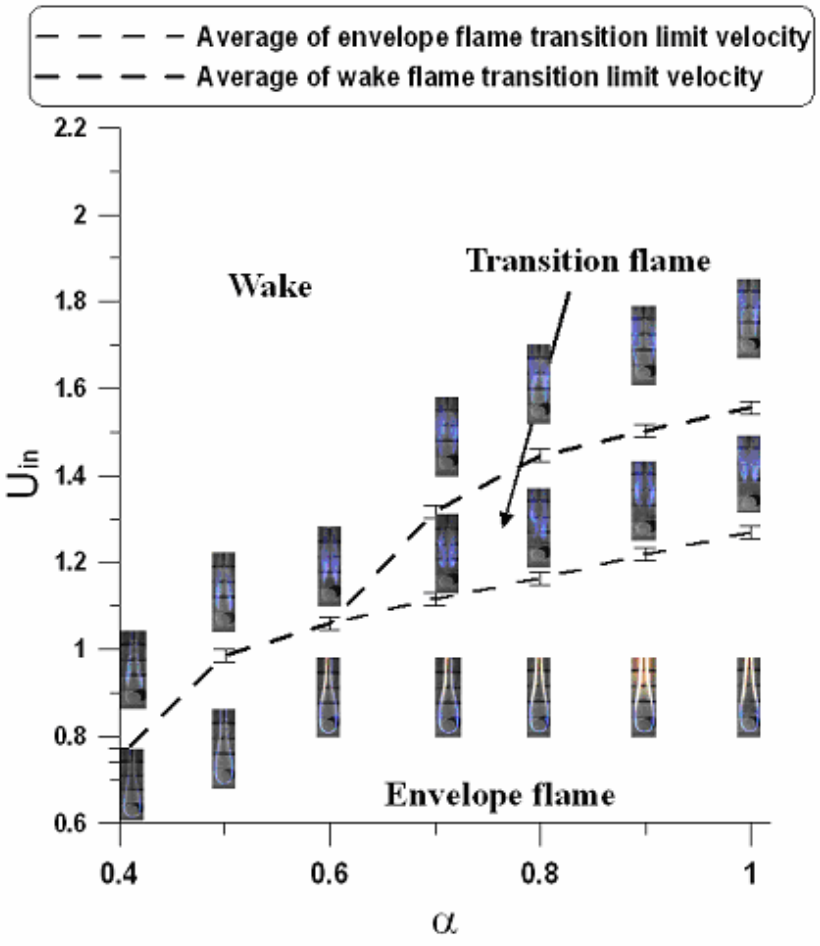

Fig. 3 the flame transition limit velocity under different α and U_{in}

It can be seen that in the higher methane mass fraction regime, ($\alpha > 60\%$), the envelop, transition and wake flames appear in order as the incoming flow velocity

increases from 0.41 to 2.63 m/sec. A transition zone between envelop and wake flame regions is identified in this regime. In such zone, the flame shows an oscillatory feature. It is highly unstable such that it might appear as a lift-off flame, wake flame or extinction. The detailed description will be given latter. On the other hand, when the methane to nitrogen mass ratio is below 60% ($\alpha \le 60\%$), the envelope flame is directly transformed into wake one as incoming velocity gradually increases up to the transition velocity, and no transition flame is identified in this regime.

4.3 Comparisons with Chang's Experiments [1]

In Chang's experiment, it investigates flame lift-off phenomenon over a cylinder burner. Its variation parameters were the incoming airflow velocity, U_{in}, and the fuel ejection velocity, V_w, respectively. The fuel used was pure methane, ejecting from the forward half part of the burn at blowing velocity, V_w=0.9~3.02 cm/s. He found that in the regime of $V_W < 0.0291$ m/s, the envelope flame will transform into wake one directly when incoming velocity gradually increases to a limiting value. On the other hand, in the regime of $V_W \ge 0.0291$ m/s., the flame structures will appear three types, envelope, wake, and lift-off flames when incoming airflow velocity, U_{in}, increases. The lift-off flame phenomenon is also found in this study under a fixed blowing velocity, V_w = 0.05m/s for pure methane fuel. In addition, this study also finds that for methane/nitrogen fuel ejected from the forward half part with V_w = 0.05m/s, in the lower methane mass fraction regime, ($Y_{CH_4} \le 0.6$), the enveloped flame is directly transformed into wake one as the transition velocity is reached. On the other hand, in the higher methane mass fraction regime, ($Y_{CH_4} > 0.6$), the lift-off flame is found between envelop and wake flame when incoming velocity gradually increases. However, It shows oscillatory feature and can only sustain for less than 8 sec, then disappears. Comparing with Chang's experiment, this study finds that the critical value and the methane mass blowing rate (ρ_{CH_4}Q, where ρ_{CH_4} is the density of methane and Q is volume rate) that lift-off flame occurs, are nearly the same for both experimental studies. Although, the measured value in this study is slightly higher than the one in Chang's experiment. However, this discrepancy is in the error range of mass flow controller. In addition, the lift-off flame always occurs at higher methane mass blowing rate. Hence, this study believes that lift-off flame is an unstable phenomenon caused by too much methane mass supply when transition velocity, where the enveloped flame is transformed into wake one, is reached.

4.4 Further Work Suggest

Several modifications are suggested for further modification of the present experiment. The particle image velocimetry (PIV) incorporates with a LASER system to generate a picture for the moving magnesium oxide particles ejected into the uniform air stream to analyze the flow pattern and flow velocity in various flame structures. The flame temperature distribution is measured by Schlieren system that can further explain the flame structure. Furthermore, to investigate the duality and hysteresis phenomena by varying the incoming airflow velocity from a higher one to lower one under different methane to nitrogen mass is also proposed.

Reference

1. C. C. Chang, Experimental Visualization of Counterflow Diffusion Flame over a Porous Cylinder, M. S. thesis, National Chiao Tung University, Taiwan, 2002.
2. C. H. Chen and S. S. Tsa, Flame stabilization over a Tsuji burner by four-step chemical reaction, *Combustion Science and Technology*, vol. 175, pp.2061-2093
3. C. H. Chen and F. B. Weng, Flame Stabilization and Blowoff Over a Porous Cylinder, *Combustion Science and Technology*, vol. 73, pp. 427-446, 1990.
4. H. Z. Chen, Experimental Visualization for Flows over the Porous Spheres and Cylinder with/without Blowing, M. S. thesis, National Chiao Tung University, Taiwan, 2004.
5. H. Tsuji and I. Yamaoka, The Counterflow Diffusion Flame in the Forward Stagnation Region of a Porous Cylinder, *Eleventh Symposium (International) on Combustion*, pp. 979-984, 1967.
6. H. Tsuji, and I. Yamaoka, The Structure of Counterflow Diffusion Flame in the Stagnation Region of a Porous Cylinder, *Twelfth Symposium (International) on Combustion*, pp. 997-1005, 1969.
7. H. Tsuji and I. Yamaoka, Structure Analysis of Counterflow Diffusion Flames in the Forward Region of a Porous Cylinder, *Thirteenth Symposium (International) on Combustion*, pp. 723-731, 1971.
8. H. Tsuji and I. Yamaoka, Structure Analysis of Anomalous behavior of methane-air and methane-hydrogen-air flames diluted with nitrogen in a stagnation flow, *Thirteenth Symposium (International) on Combustion*, pp. 145-152, 1992.
9. H. Tsuji and S. Ishizuka, An Experimental Study of Effect of Inert Gas on Extinction of Lamina Diffusion Flames, *Eighteenth Symposium (International) on Combustion*, pp. 695-703, 1981

國立交通大學博士班研究生
出席國際會議研究心得報告

報告人姓名	張文奎	報告日期	94年8月31日
系所及年級	機械系博三	核定文號	94年6月6日　05D099
連絡電話	0937226555	電子信箱	popinjay.me91g@nctu.edu.tw
會議期間	94.8.29–94.9.1	會議地點	捷克布拉格
會議名稱	（中文）第十六屆傳輸現象國際會議 （英文） The Sixteenth International Symposium on Transport Phenomena		
發表論文題目	（中文）火焰在有限長度PMMA燃料及伴隨熱輻射效應下傳播情形之實驗與數值模擬 （英文）Experimental and Numerical Studies for Flame Spread over a Finite-Length PMMA with Radiation Effect		

報告內容包括下列各項：

一、參加會議經過：

第十六屆傳輸現象國際會議於8月29日~9月1日在捷克的捷克技術大學舉辦，來自各國的學生、教授以及公司的研究人員踴躍參與此次的研討會，會議人數將近200人，會議總共四天，第一天早上八點到會場辦理報到手續並且領取會議相關資料，會議開始依據不同的燃燒研究領域安排大型會議廳發表研究成果，由各論文作者依表列次序上台發表，晚上舉行接待茶會，讓與會者彼此認識與交換研究心得。學生論文發表被安排在第三天下午三點半發表，經過會議主持人簡短的介紹，學生上台開始十五分鐘的口頭報告，報告完畢後有五分鐘的討論，會後討論熱烈，學生也盡力回答在座先進的問題。

二、與會心得：

在個人發表研究成果之餘，亦參加了會議中數個與個人研究領域相關的議程，並聽取各地學者專家所發表的研究成果及看法。此次參與國際學術會議令學生獲益良多，也認識了一些國外學者與博士班學生，在會議中交換了不同的看法與意見，學習到許多不同的觀點與學習精神，讓自己在本研究領域中有更進一步的了解，相信對未來的研究會有相當大的幫助。

三、建議：

學生此次出國參加國際學術會議，深深覺得國內的研究規模，論文質與量，雖每年均有進步，但是與美、日比較仍有一段差距。希望學術界宜鼓勵較基礎之研究以提昇我國學術地位，並支援工業界以產品開發導向的研究，讓學術單位與產業界能夠充份配合，以達學以致用的目的。另外也希望往後參加國際學術會議的研究生盡量以口頭報告方式上台報告，一方面能夠訓練英文演講能力，另一方面也能訓練表達能力。

四、攜回資料名稱與內容：

會議論文集一本及會議論文光碟一份。

EXPERIMENTAL AND NUMERICAL STUDIES FOR FLAME SPREAD OVER A FINITE-LENGTH PMMA WITH RADIATION EFFECT

Wen-Kuei Chang and Chiun-Hsun Chen*, Ton-Min Liou**
***Department of Mechanical Engineering, National Chiao Tung University**
Hsinchu, Taiwan 30050, R.O.C.
****Department of Power Mechanical Engineering, National Tsing Hua University**
Hsinchu, Taiwan 30050, R.O.C.

Keywords: *Ignition delay; Downward flame spread; PMMA; radiation effect*

Abstract

The phenomena of ignition delay and subsequent downward flame spread over a finite length PMMA slab under an opposed flow with radiation effect are investigated by using an unsteady combustion model. The corresponding experimental test channel is 700 mm long with $100 \times 100 mm^2$ rectangular cross section. The specimens are mounted on the groove of the test section and the groove sides are covered with asbestos plates. The thermocouples and laser holographic interferometer are used to measure the surface and gas temperatures, respectively. The simulated results indicate that the ignition delay time increases as the opposed flow velocity and solid fuel thickness increase and the opposed flow temperature decreases. On the other hand, the ignition delay time becomes longer when the radiation effect is considered. The flame spread rate increases as the opposed flow velocity and solid fuel thickness decrease and the opposed flow temperature increases. However, the influence of radiation effect on the flame spread rate is not significantly. Furthermore, a comparison between the predictions of Wu's model [1] and present model is given. The downstream size of flame still grows in Wu's model, whereas it contracts over the solid fuel surface in this work due to the finite length solid fuel. As a consequence, the flame spread rate in present model becomes lower and is closer to the experimental measurement. The predicted flame spread rate and temperature distribution have an excellent quantitative agreement with the measurements in high velocity regime. However, the discrepancies between the predicted and experimental results increase in the lower velocity regime. The main reason is believed to the 3D effect, which is not considered in the present simulation.

1 Introduction

This work investigates the ignition and subsequent flame spread characteristics over a finite length of thick solid fuel under a mixed convection condition using an unsteady combustion model with radiation effect in a two-dimensional wind tunnel. It is motivated from a previous work [1], which only considered the ignition and flame spread over an infinite-length fuel plate in an open atmosphere without radiation. In that work, the deviations in predicted flame spread rates from the corresponding experimental measurements were attributed to these effects mentioned above. Therefore, an extensive modification in the unsteady combustion was carried out to mitigate the discrepancy between the predictions and measurements.

Sibulkin et al. [2] investigated the effects of gas phase and surface radiation on the burning of vertical fuel surfaces. It was found that gas phase radiation has a negligible effect on burning rate, whereas the surface radiation strongly affects the combustion. West et al. [3] studied the surface radiation effects on flame spread over thermally thick fuels in an opposing flow. They concluded that the fuel surface radiation is important for thermally thick fuel at all flow levels, however, and it is important for thermally thin fuel only at low velocity level. Rhatigan et al. [4] investigated the gas phase radiative effects on the burning and extinction of a solid fuel.The computed results indicated that the gas radiative effects are more pronounced at low stretch rates. They also developed a computationally more efficient gray gas model, using a calibrated correction factor for the mean absorption coefficient. It is found that many of the flame characteristics can be computed with sufficient accuracy despite the difference in radiative structure. Lin and Chen [5] investigate how the gas-phase radiation, whose model includes both the cross-stream and stream-wise gas phase radiation coupled with solid phase one, affected the spreading flame. By comparing the results with the predicted ones of Chen and Cheng [6], which only considered the radiation effect in cross-stream direction, they concluded that the stream-wise radiation contributes to reinforce the forward heat transfer rate subsequently increasing the flame spread rate.

Pan [7] and Chen [8] investigated the steady flame spread characteristics over PMMA in an opposed forced convection environment in a

wind tunnel. The variable parameters were the velocity and the temperature of flows and the thickness of fuel. They found that flame spread rate increases with an increase of the temperature of flow, a decrease of the flow velocity or the thickness of fuel. Their image results further demonstrated that the thermal boundary layer becomes thicker when the temperature of incoming flow is higher under a fixed flow velocity or the incoming flow velocity is slower at the same flow temperature. Wu et al. [1] developed an unsteady combustion model with mixed convection to investigate the flame spread behaviors of a thick PMMA slab with an infinite length in an opposed flow environment. Simulation results of flame spread rate were compared with the measurements obtained by Pan [7]. The agreements were well in general except at the low-speed flow regime. In addition, this numerical study indicated that the ignition delay time increases with an increase of the opposed flow velocity or a decrease of the opposed flow temperature. The ignition delay time is almost constant at a low opposed flow velocity. Nakamura [9] numerically studied the enclosure effect on flame spread over solid fuel in microgravity. Because the confinement of the flow field and the thermal expansion initiated by heat and mass addition in the chamber, the flame spread rate for the case with enclosure is faster than the one without any enclosure. The predictions also showed that the enclosure effect is more significant at the low flow velocity condition and becomes less important with increasing imposed flow velocity. Fujita et al. [10] experimentally studied the radiative ignition on paper sheet in microgravity. The results showed that the gas phase temperature becomes higher than that of the solid surface before ignition, and the main mechanism of radiative solid ignition here is due to the gas phase reaction. Furthermore, the ignition delay time strongly depends on the oxygen concentration and ambient pressure. It decreases with a higher oxygen concentration or ambient pressure.

Kumar et al. [11] used a two dimensional flame spread model with flame radiation to compare the extinction limits and spreading rates in opposed and concurrent spreading flames over thin solids. The varying parameters were oxygen percentage, free stream velocity, and flow entrance length. Numerical results showed that at low free stream velocities with shorter entrance length, the flame spread rates are higher and have a lower oxygen extinction limit, whereas in high free stream velocities, the flame spread rates are lower and have a higher oxygen extinction limit. The flame spread rate in opposed flow varies with free stream velocity in a non-monotonic manner, with a peak rate at an intermediate free stream velocity. The flame spread rate in concurrent flow increases linearly with free stream velocity. Kumar et al. [12] also presented a numerical study on flame-surface radiation interaction in flame spread over thin solid fuels in quiescent microgravity and in normal gravity environments. It was observed that the flame in microgravity is very sensitive to the surface radiation properties. The fuel with high solid absorptivity can absorb substantial flame radiation and flame spreads faster than the corresponding adiabatic case irrespective of value of solid emissivity.

As mentioned previously, the modifications of present work from the original combustion model of Wu et al. includes the several effects, such as the enclosure, the finite-length fuel plate and the radiation. The entire process from ignition to subsequent flame spread will be examined and depicted in detail, and the simulated results will compare with the predictions of Wu et al. [1] and the measurements of Pan's experiment [7].

2 Mathematical Model

Figure 1 illustrates the physical configuration of two-dimensional ignition over a vertically oriented thick solid fuel in a mixed convective environment. The test section of wind tunnel is 70 cm long with 10 cm height. The solid fuel plate used in present simulation is 30 cm long and the thicknesses are 0.82 cm and 1.74 cm, respectively, which are exactly the same as those used in Pan's experiments [7]. For $t < 0$, a steady flow in wind tunnel is built up in advance over entire test section. As $t \geq 0$, an external heat flux in Gaussian distribution, in which the width is 0.5 cm with a peak value of 5 W/cm^2, is

imposed on the solid surface. Its center is aimed at x=0, the connecting point between the solid

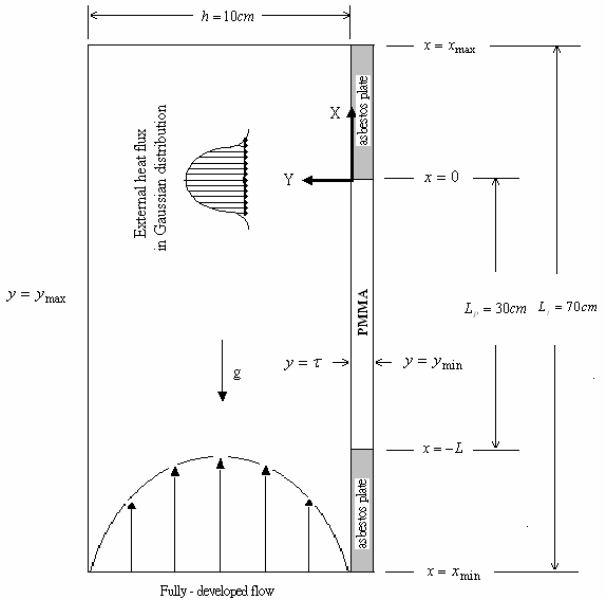

Fig. 1. The schematic of flame spread over a thick PMMA slab in the mixed air flow in a wind tunnel.

fuel and adiabatic plate. In other words, only half of the radiation energy is used to heat up the PMMA fuel directly.

The unsteady combustion model basically is modified from that developed by Lin and Chen [13]. Also, a radiation model developed by Wu and Chen [14] is adopted in this unsteady combustion model. The mathematical model consists of both gas- and solid-phase equations, which are coupled together at the interface. The corresponding assumptions and normalization procedure can be found in Wu [15] and are not represented here for brevity. The numerical scheme adopts the SIMPLE algorithm [16]. The unsteady governing equations as well as the interface and boundary conditions are solved at each time step until a convergence criterion (residual < 0.01) is satisfied. After that, they are marched to the next time step. Computations are carried out on non-uniform mesh distribution. The smallest grid size is 0.01 cm. Grid points are most clustered in external radiative heating region to capture the drastic variations in the flame, the grids then expand upstream and downstream. A grid-size independence test was conducted in advance, and the selection of non-dimensional time step of $\Delta t = 10$ (equivalent to real time 0.02 s) and non-uniform grid distribution of 290×95 was found to achieve an optimal balance among the solution resolution, computational time and memory space requirements. The computational time for a case is typically about 4 days on a PC at National Chiao Tung University.

3 Results and Discussion

In order to make the fair comparisons with Pan (1999) and Wu et al. [1], the parametric studies are performed by changing the opposed flow velocity and the flow temperature, respectively, which are also the same as those in experiments of Pan [7]. A comparison between the predictions of Wu's model [1] and present model will be given first. Note that in the simulation of Wu et al. [1], the fuel slab is extended infinitely in both directions, the ignition/combustion is in an open atmosphere and the radiation effect is not considered.

Figure 2 shows the ignition delay time versus the opposed flow temperature under three different opposed flow velocities for $\overline{u_\infty} = 40$ cm/s, 70cm/s, and 100cm/s, and the solid fuel thicknesses are 0.82 cm and 1.74 cm, respectively. Remind that the present simulation includes the consideration of radiation effect. The values expressed by solid lines are the ignition delay times for $\bar{\tau} = 0.82$ cm, whereas the ones by dashed lines are for $\bar{\tau} = 1.74$ cm. In this figure, it can be seen with an increase of the incoming flow velocity. This is because that the thermal boundary layer becomes thinner in the higher opposed flow velocity regime, which carries more produced fuel vapors to the downstream to make the accumulation of fuel vapor near the solid fuel surface to become more difficult that increases the formation time of the flammable mixture and so delays the ignition. On the other hand, with a fixed incoming flow velocity, the ignition delay time decreases with an increase of the incoming flow temperature. This is because that the higher temperature flow can heat the solid fuel more effective to generate more fuel vapors to form the flammable mixture earlier, as a consequence, to shorten the ignition time. Furthermore, the ignition delay time for $\bar{\tau} = 1.74$ cm is longer than the one for

$\bar{\tau} = 0.82$ cm under the fixed flow velocity and

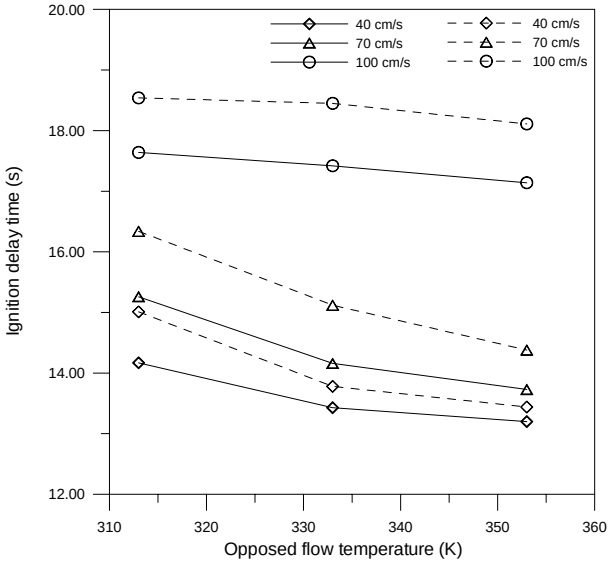

Figure 2. Ignition delay time versus the opposed flow temperature under different opposed flow velocity for $\bar{\tau} = 0.82cm$ (by solid lines) and $\bar{\tau} = 1.74cm$ (by dashed lines),respectively.

temperature. Comparing with the thinner solid fuel, the thicker one has greater thermal inertial that requires more energy to reach the ignition temperature, increasing the ignition delay time. The above trends have been confirmed by the predictions of Wu et al. [1] and Wu [15] and the experimental observations of Pan [7], Chen [8].

Figure 3 presents the ignition delay time as a function of the opposed flow temperature under a fixed flow velocity ($\overline{u_\infty} = 40$ cm/s) with and without radiation effects. In general, the ignition delay time decreases with an increase of the opposed flow temperature no matter what the effect of radiation is considered or not. However, the ignition delay time without radiation effect is shorter than the one with radiation effect. It can be explained as follow. Figure 4 displays the distributions of heat fluxes along the solid fuel surface at the instant just before ignition ($\bar{t} = 13.72s$). q_{ex} and q_c are the external input radiant heat flux in Gaussian distribution and the conduction heat flux from the gas, and the gas phase radiation feedback and radiation heat loss from the solid fuel surface are represented by q_{gr} and q_{sr}. The sum of total heat fluxes is the net heat flux on the solid fuel surface, q_{net}. The positive value indicates the solid fuel gains energy from the gas phase and the negative one

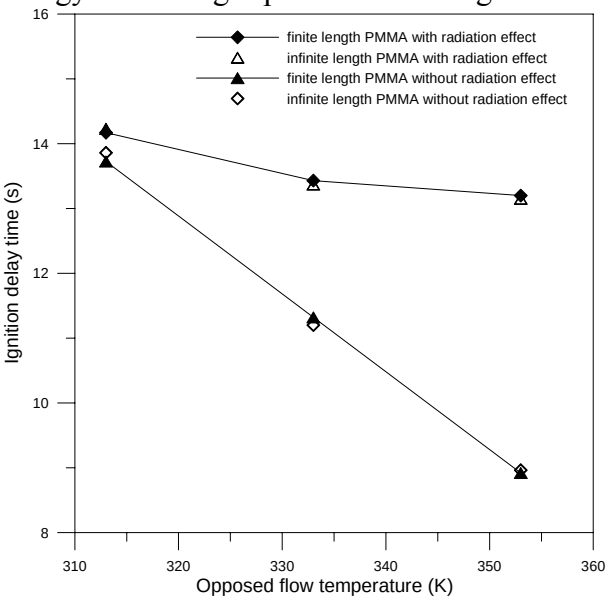

Fig. 3. Ignition delay time versus the opposed flow temperature under a fixed opposed flow velocity $\overline{u_\infty} = 40cm/s$ with and without radiation effect, respectively.

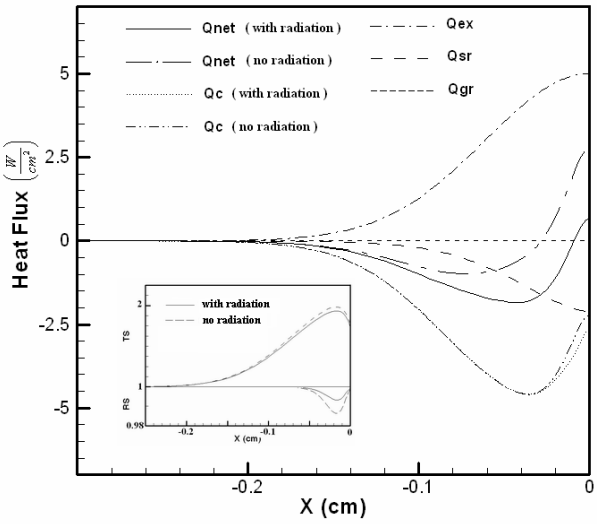

Fig. 4. The distribution of heat fluxes along the solid fuel surface at $\bar{t} = 13.72s$, $\overline{T_i} = 313K$, $\overline{u_\infty} = 40cm/s$ with and without radiation effects, respectively.

represents the heat loss from the solid fuel surface. From this figure, it can be found that the net heat flux (q_{net}) near the origin is higher in the case without radiation effect. The solid fuel can receive more energy for pyrolysis and produces the fuel vapor more effective, shorting the formation time of flammable mixture. Therefore, the ignition becomes faster without the radiation effect. The inset of Figure 5 shows the

distributions of solid fuel temperature and density contours at the instant just before ignition. Comparing with the case with radiation effect, it can be seen that the solid fuel temperature is higher such that pyrolyzes more fuel vapor when the radiation effect is not considered. Intensive pyrolysis also makes the gas phase chemical reaction rate increase. Note that the peaks of the temperature and density distributions are not exactly at the origin but shifted slightly. It is because that the solid fuel tip not only receives the energy from the external input heat flux but losses heat to the ambient simultaneously.

Furthermore, comparing the ignition delay times with and without radiation in Fig. 3, the differences between them increase with an increase of the incoming flow temperature. It is because the radiation heat loss from the solid fuel surface becomes greater as the incoming flow temperature increases. The surface temperature becomes higher when the solid fuel is immersed in a hotter flow. Since q_{sr} is proportional to T_s^4, the radiation heat loss from the solid fuel surface to the ambient becomes greater. In other words, the solid fuel needs more time to receive more energy to rise its temperature for pyrolysis. Therefore, the ignition delay time in the case with radiation effect increases with an increase of incoming flow temperature. Regarding the effect of solid fuel length on ignition delay time, the difference between the finite and infinite lengths is insignificant. This is because that the ignition delay time is dominated mainly by the incoming flow velocity and temperature and the solid fuel thickness, but not length.

Figures 5a and 5b display the flame spread rate as a function of the incoming flow temperature under three different flow velocities for solid fuel thickness of 0.82 cm and 1.74 cm, respectively. The solid and dashed lines display the simulated results by the present work and the predictions of Wu's model [1], respectively, and the symbols show the measured data of Pan [7]. It can be found that the flame spread rate increases with an increase of flow temperature under a fixed incoming flow velocity. The reason can be explained as follow. From the Figs. 6a(a), 6b(a) and 6c(a), which illustrate the temperature contours of gas and solid phases and vector distribution under a fixed opposed flow velocity of $\bar{u}_\infty = 40cm/s$ and the opposed flow temperatures are 313K, 333K and 353K, respectively. As expected, hotter opposed flow leads to a stronger flame. For example, the non-dimensional maximum flame temperatures are 5.3624, 5.4195 and 5.5168 for the incoming flow temperatures of 313K, 333K and 353K, respectively. The solid fuel receives more energy from the stronger flame, enhancing the upstream pyrolysis length (and the preheat length) and intensity that shortens the formation time of flammable mixture ahead of the flame front. Consequently, the flame spread rate becomes faster with a higher flow temperature. As to the effect of incoming flow velocity, it can be found that the flame spread rate decreases with an increase of incoming flow velocity under a fixed flow temperature. This is because that the higher incoming flow velocity increases the flame stretch. In the meantime, the heat transfer from the flame front to preheat the solid fuel becomes more difficult and the most of fuel vapors generated from the pyrolysis zone are carried to downstream. These factors results in a weaker flame that the corresponding flame spread rate becomes lower. The mentioned phenomena can be observed from the Fig.s 6a(a), 6d(a) and 6e(a), which are for different incoming flow velocity varied form 40 cm/s to 100 cm/s and the flow

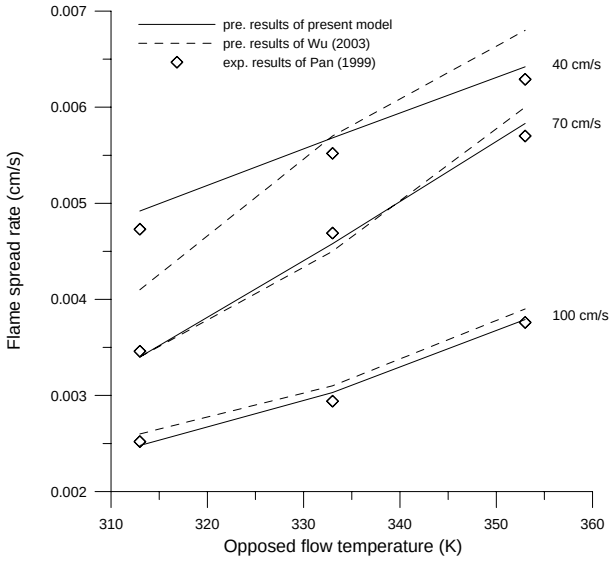

Fig. 5a. The flame spread rate versus the opposed flow temperature under different opposed flow velocity for $\bar{\tau} = 0.82\,\text{cm}$.

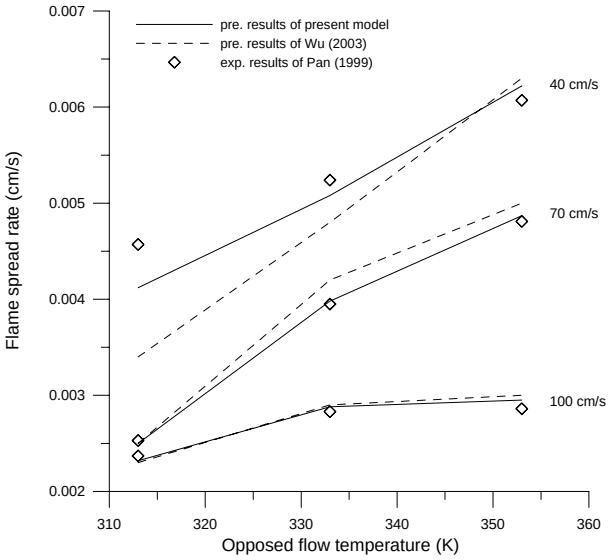

Fig. 5b. The flame spread rate versus the opposed flow temperature under different opposed flow velocity for $\bar{\tau} = 1.74\,\text{cm}$.

temperature is fixed at 313K.

For the effect of solid fuel thickness, it is found that the flame spread rate decreases with an increase of solid fuel thickness at the same incoming flow velocity and temperature. This is because the thicker solid fuel has greater thermal inertial that needs more energy to rise its own temperature to pyrolyze that needs more time to form the flammable mixture and results in a lower flame spread rate. Figures 6a(a)-6e(a) and 6a(c)-6e(c) are for solid fuel thickness 0.82cm and 1.74cm under different opposed flow velocities and temperatures. They also show that the flame spread is faster for the thinner solid fuel. The flame size and upstream preheated area are all greater in the thinner ones. The above trend has been confirmed by the predictions of Wu et al. [1] and West [3] and the experiments of Pan [7], Chen [8].

Comparing with the simulated results of Wu et al. [1] in the Figures 5a and 5b, the predictions of present model are closer to the Pan's experimental measurements [7]. It can be explained as follow. Figures 6a(b)-6e(b) present the temperature contours of gas and solid phases and vector distribution under different opposed flow velocities and temperatures for solid fuel thickness is 0.82cm. Remind that the radiation effect is not under consideration in these cases. Comparing the gas phase temperature contours in Fig. 6a(a) and 6a(b), the non-dimensional maximum flame temperatures are 5.3624 and 5.8236, respectively. The upstream preheated area of solid fuel is longer in the case without radiation effect. It indicates that the heat loss from solid fuel is reduced and it gains more energy from the stronger flame and enhances the pyrolysis intensity. The downstream size of flame still grows in Wu's simulation, whereas the present one contracts slightly over the fuel surface and the downstream flame temperature decreases. The formation time of flammable mixture becomes longer, resulting in a lower downward flame spread. However, this phenomenon becomes insignificantly when the flow temperature increases.

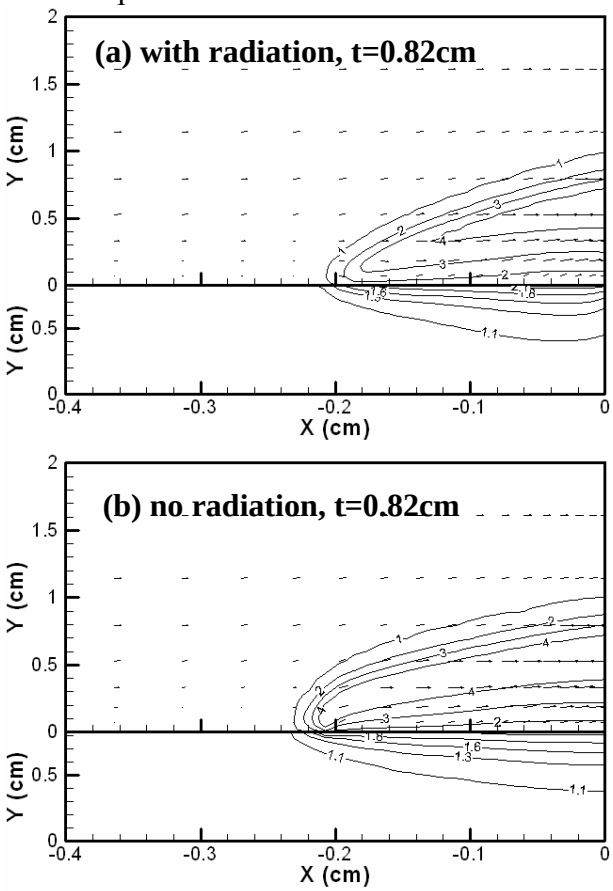

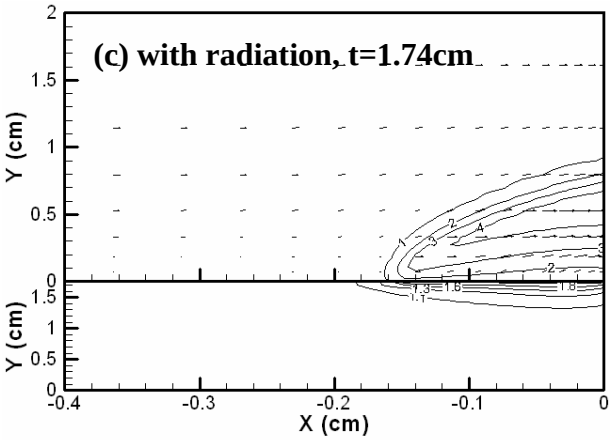

Fig. 6a. The gas-solid phases temperature contours and vector distribution at $\bar{t} = 25s$, $\overline{T}_i = 313K$ and $\bar{u}_\infty = 40cm/s$.

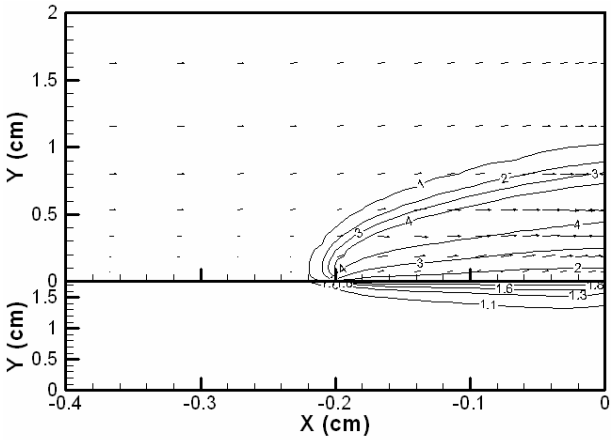

Fig. 6b. The temperature contours of gas and solid phases and vector distribution at $\bar{t} = 25s$, $\overline{T}_i = 333K$ and $\bar{u}_\infty = 40cm/s$.

4 Conclusions

This work utilizes an unsteady radiation combustion model, using the incoming flow velocity and temperature and the solid fuel thickness as parameters, to investigate their effects on the ignition delay and the subsequent downward flame spread over a finite length PMMA slab under a mixed convection condition in a wind tunnel. The simulated results of present work are compared with the corresponding simulated predictions and experimental measurements. In general, the qualitative trends between the present predicted results and the experimental measurements are the same. It is found that the ignition delay time increases with an increase of incoming flow velocity, the solid

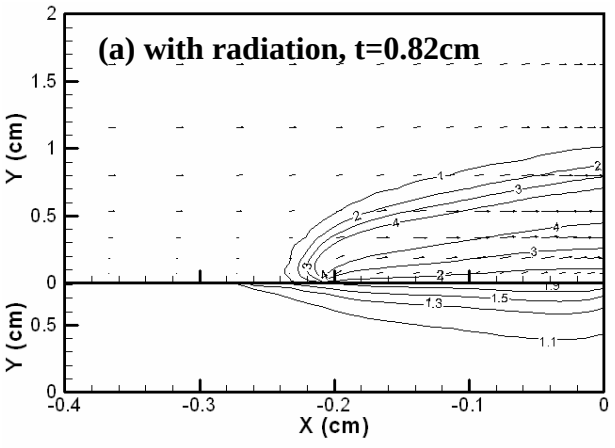

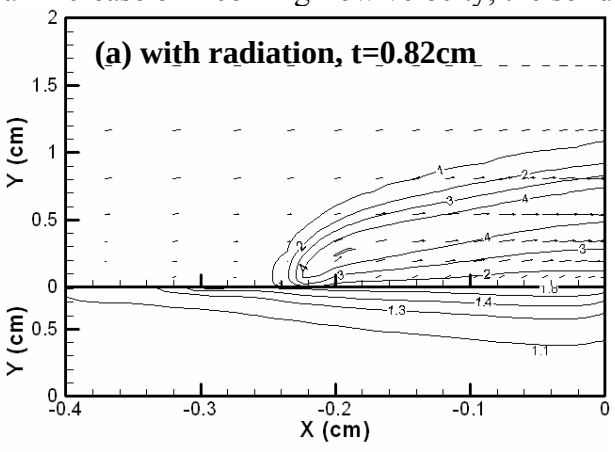

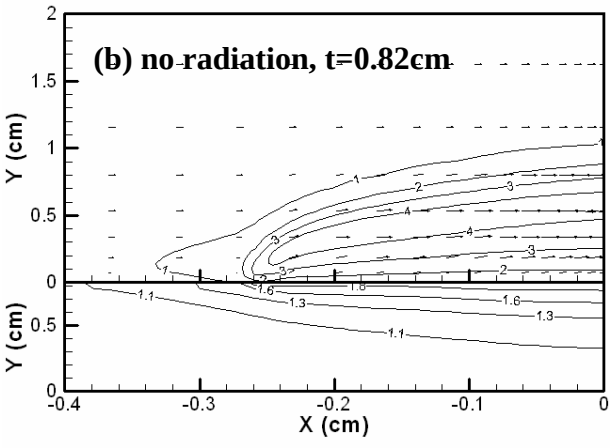

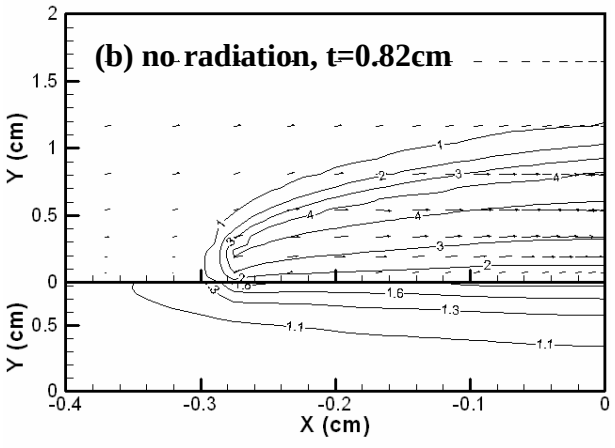

(c) with radiation, t=1.74cm

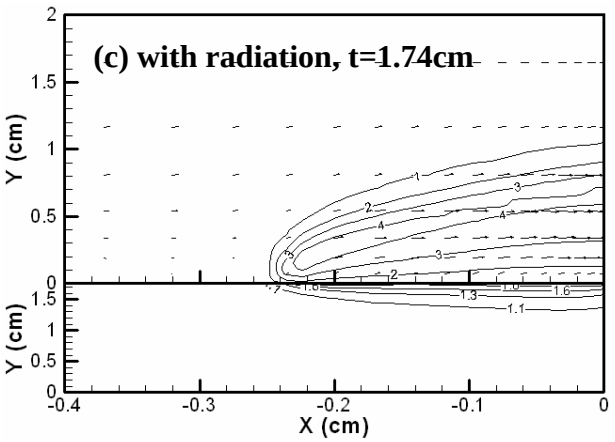

Fig. 6c. The temperature contours of gas and solid phases and vector distribution at $\bar{t} = 25s$, $\bar{T}_i = 353K$ and $\bar{u}_\infty = 40cm/s$.

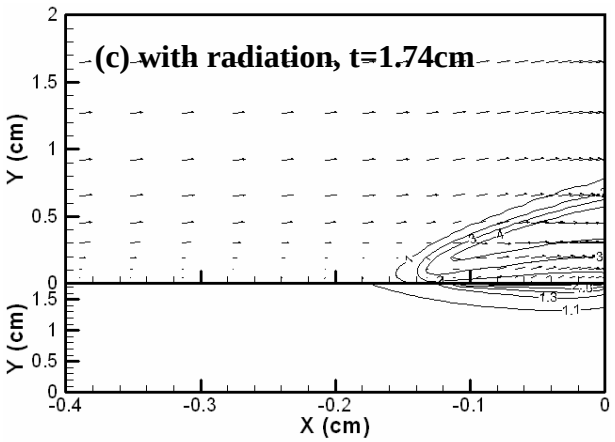

Fig. 6d. The temperature contours of gas and solid phases and vector distribution at $\bar{t} = 25s$, $\bar{T}_i = 313K$ and $\bar{u}_\infty = 70cm/s$.

fuel thickness and a decrease of flow temperature. The ignition delay time with radiation effect takes longer than the one without radiation effect. Furthermore, the differences of the ignition delay time between with and without radiation effects increase when the flow temperature becomes higher under a fixed incoming flow velocity. The flame spread rate

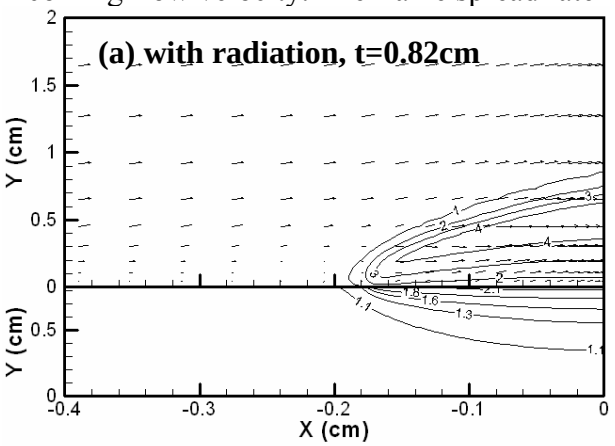

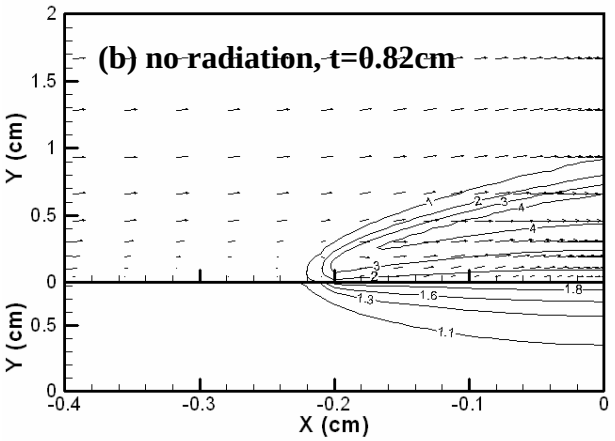

increases with a decrease of the incoming flow velocity and solid fuel thickness, and an increase of the flow temperature. The radiation effect in the lower flow velocity regime is found more effective. The downstream flame size still grows over an infinite length fuel plate, whereas the present one contracts over a finite length fuel plate. The effects of gas phase radiation and

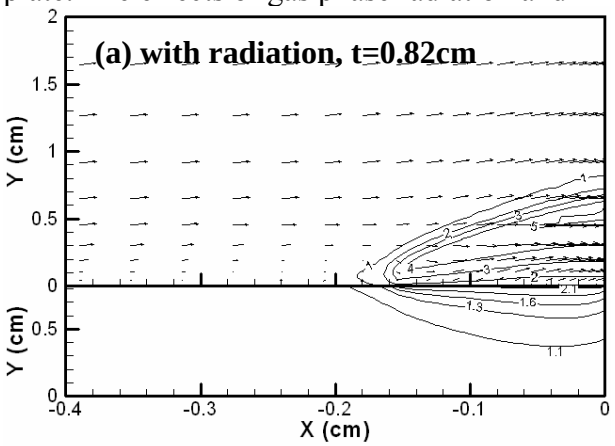

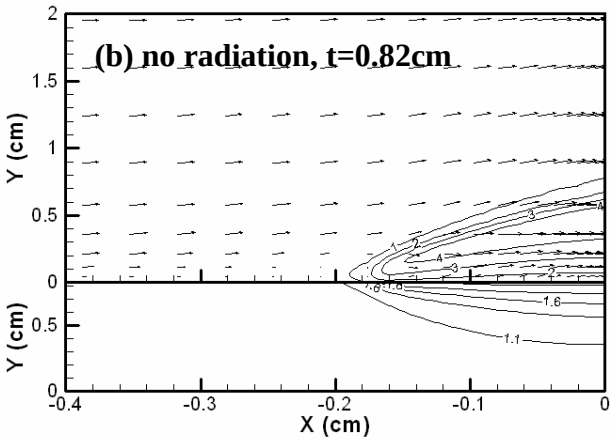

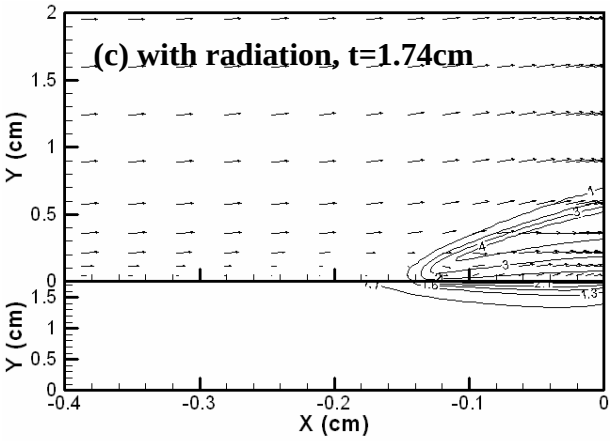

Fig. 6e. The temperature contours of gas and solid phases and vector distribution at $\bar{t} = 25s$, $\bar{T}_i = 313K$ and $\bar{u}_\infty = 100cm/s$.

finite fuel length mentioned above result in a lower flame spread rate, so that they mitigates the discrepancies between the present simulated predictions and the experimental measurements. The predicted flame spread rates have an excellent quantitative agreement with the ones by experimental measurements. However, it still exists a discrepancy at low velocity regime. The main reason can be attributed to the 3D effect which is not included in the present two dimensional model.

Reference

[1] Wu, K. K., Fan, W. F., Chen C. H., Liou, T. M. and Pan, I. J. Downward Flame Spread Over a Thick PMMA Slab in an Opposed Flow Environment: Experiment and Modeling, Combustion and Flame, Vol. 132, pp 697-707, 2003.

[2] Sibulkin, M., Kulkarni, K. and Annamalai, K. Effect of Radiation On The Burning of Vertical Fuel Surfaces, Eighteenth Symposium (International) on Combustion, The Combustion Institute, pp 611-617, 1981.

[3] West, J., Bhattacharjee, S. and Altenkirch, R. A. Surface Radiation Effects on Flame Spread Over Thermally Thick Fuels in an Opposing Flow, Transactions of the ASME, Vol. 116, pp 646-651, 1994.

[4] Rhatigan, J. L., Bedir, H. and T'ien J. S. Gas-Phase Radiative Effects on the Burning and Extinction of a Solid Fuel, Combustion and Flame, Vol. 112, pp 231-241, 1998.

[5] Lin, T. H. and Chen, C. H Influence of Two Dimensional Gas Phase Radiation on Downward Flame Spread, Combustion Science and Technology, Vol. 141, pp 83-106, 1999.

[6] Chen, C. H. and Cheng, M. C. Gas Phase Radiative Effects on Downward Flame Spread in Low Gravity, Combustion Science and Technology, Vol. 97, pp 63-83, 1994.

[7] Pan, I. J. Experimental Analyses of Flame Spread Behavior Over Solid Fuel Under Opposed Flow, MS thesis, National Tsing Hua University, Hsinchu, Taiwan, R. O. C., 1999.

[8] Chen, R. J. Experimental Analyses of Flame Spread Behavior Over Solid Fuel Under Suddenly Opposed Flow, MS thesis, National Tsing Hua University, Hsinchu, Taiwan, R.O.C., 1999.

[9] Nakamura, Y., Kashiwagi, T., Mcgrattan, K. B. and Baum, H. R. Enclosure Effects on Flame Spread Over Solid Fuels in Microgravity, Combustion and Flame, Vol. 130, pp 307-321, 2002.

[10] Fujita, O., Takahashi, J. and Ito, K. Experimental Study on Radiative Ignition of A Paper Sheet in Microgravity, Proceedings of the Combustion Institute, Vol. 28, pp 2761-2767, 2000.

[11] Kumar, A., Shin, H. Y. and T'ien, J. S. A Comparison of Extinction Limits and Spreading Rates in Opposed and Concurrent Spreading Flames Over Thin Solids, Combust. Flame, Vol. 132, pp 667-677, 2003.

[12] Kumar, A., Tolejko, K. and T'ien, J. S. A Computation Study on Flame Radiation-Surface Interaction in Flame Spread Over Thin Solid-Fuel, The 6th ASME-JSME Thermal Engineering Joint Conference, 2003.

[13] Lin, P. H. and Chen, C. H. Numerical Analyses for Radiative Autoignition and Transition to Flame Spread Over A Vertically Oriented Solid Fuel in A Gravitational Field, Combustion Science and Technology, Vol. 151,pp 157-187, 2000.

[14] Wu, K. K. and Chen, C. H. Radiation Effects For Downward Flame Spread Over A Thermally Thin Fuel In A Partial-Gravity Environment, Combustion Science and Technology, Vol. 176, pp 1909-1933, 2004.

[15] Wu, K. K. A Study of Flame Behaviors over a Solid Fuel in a Natural Convection Environment. Ph.D. Dissertation, National Chiao Tung University, Hsinchu, Taiwan, R.O.C., 2003.

[16] Patankar, S. V. Numerical Heat Transfer and Fluid Flow, McGraw-Hill, New York, 1980.